RSC Advances

ROYAL SOCIETY OF CHEMISTRY

www.rsc.org/advances

Journal Name

ARTICLE

Electrocatalytic reduction of coreactant by hemin-graphene-Au nanoparticles ternary composite for sensitive electrochemiluminescent cytosensing

Received 00th January 20xx,
Accepted 00th January 20xx

DOI: 10.1039/x0xx00000x

www.rsc.org/

Xiaoyan Xin [a,b], Yiying Yang [c], Jing Liu [b], Xiaomeng Wang[b], Hong Zhou [a,b,*], Bing Yu [c,*]

A ternary composite of hemin-reduced graphene oxide-Au nanoparticles (H-RGO-Au) was synthesized with a higher electrocatalytic activity for the reduction of hydrogen peroxide than that of hemin-graphene components and was used as a catalyst to initiate sensitive electrochemiluminescent (ECL) quenching of quantum dots (QDs) due to the electrocatalytic reduction of coreactant H_2O_2. Based on this and specifically recognization between concanavalin A (Con A) and mannose or N-glycans on the cell surface, an ultrasensitive cytosensing for 5 cancer cells detection was first proposed. The designed strategy showed an expansive application for the construction of versatile ECL cytosensing platforms for many important biomolecules.

Introduction

Since the first Electrochemiluminescent (ECL) phenomena was found from silicon-quantum dots (QDs) in 2002,[1] QDs-based ECL-sensing strategies have been improved quickly with its gradually-emerging advantages such as low background, high sensitivity and controllability.[2-5] Most sensitive ECL biosensors involve coreactant consumption using an enzymelinked probe.[6-8] However, during the preparation of enzymelinked probe, the misgivings of denaturation and complex purification process greatly limited the practical applications of these reported natural enzymes probes.[9] Therefore, another promising enzyme mimics ECL probe with excellent performances has drawn considerable interest recently and developed rapidly. The advantages of enzyme mimics probe, such as stable against denaturing, high electrocatalytic reactivity, convenience for storage and treatment, show excellent performances in sensing process.[10,11]

Recently, nanomaterial enzyme mimics based on graphene oxide (GO) has become a widely utilized promising material and shown impressive catalytic performance for the reasons that GO provide large specific surface areas and high adsorption capacity, which makes it to be good a substrate for heterogeneous catalytic processes.[12-14] For examples, using GO as substrate to synthesis all kinds of metallic nanoparticles include Au NPs or Au-Pd bimetallic nanoparticles,[15,16] and Fe_3O_4 magnetic nanoparticles.[17] These hybrid nanomaterials were reported to demonstrate a synergistic catalytic capacity with high peroxidase-like activity and were employed for cancer cell detection. Up to now, the reported graphene-based hybrid peroxidase mimetics are mainly diplex, such as hemin-RGO. Hemin is known to be the activate site in peroxidase and exhibits the peroxidase-like activity. And RGO is expected to be a good substrate for heterogeneous catalytic processes due to high adsorption capacity and excellent electrical conductivity.[18] However, higher catalytic capacity is required during the detection of low-abundance biological samples. Also these diplex compound are in face of complicated modification process when combined with other assistant nanomaterial, for example Au NPs.[19] Additionally, the current traditional electrochemical method which was used in application of above material for sample detection still showed some problems including high background and unsatisfactory sensitivity. Weng et al recently report an interesting ternary graphene-family composite which showed excellent catalytic activity for decomposition of hydrogen peroxide. Further application of this ternary composite on detection of cancer biomarker or cancer cells holds promising prospects.[20]

In this article, by virtue of QDs-based ECL method, a simple but sensitive ECL cytosensor was first designed using a ternary composite of hemin-reduced graphene oxide-Au nanoparticles (H-RGO-Au) as a novel mimetic peroxidase with high electrocatalytic activity for the reduction of H_2O_2. In situ introduction of Au NPs in the hybrid nanomaterial avoided complex modification process and further increased the catalytic activity of grapheme-family composite due to the synergistic effect from GO, hemin and Au nanoparticles.The designed ECL biosensor could specifically recognize and bind to N-glycans on the cell surface for novel ultrasensitive

[a] Collaborative Innovation Center of Functionalized Probes for Chemical Imaging in Universities of Shandong, Shandong Normal University, Jinan 250014, P. R. China
[b] School of Chemistry and Chemical Engineering, Linyi University, Linyi 276005 (P. R. China). Email: zhouhong830215@126.com; Fax: (+86)-539-8766867.
[c] College of Chemical and Environmental Engineering, Qingdao University, Qingdao, 266071 (P. R. China). Email: yubingqdu@163.com.

cytosensing due to the loaded Con A. Owing to the good performance of the designed ternary composite H-RGO-Au and the combination of ECL biosensing technology, this proposed method could sensitively detect K562 cells with a linear calibration ranged from 4.8×10^2 to 5.0×10^5 cells mL^{-1}.

Experimental

Reagents and apparatus

Poly (diallyldimethylammonium chloride) (PDDA), Concanavalin A (Con A), Nacetylglucosamine (GlcNAc) and mannose (Man) were purchased from Sigma-Aldrich. $NaBH_4$, ascorbic acid (AA), 3-Mercaptopropionic (MPA) and $HAuCl_4$ were obtained from Shanghai Reagent Co., Ltd. (Shanghai, China). Graphene oxide was gotten from Nanjing XFNANO Materials Tech Co., Ltd. Hematin Chloride was from Shanghai Generay Biotech Co., Ltd. $Cd(NO_3)_2 \bullet 4H_2O$, CTAB, $Eu(NO_3)_3$, $Na_2S \bullet 9H_2O_2$ and other reagents were obtained from Aladdin. All aqueous solutions were prepared using ultra-pure water.

The electrochemical and ECL emission measurements were conducted on a MPI-A multifunctional electrochemical and chemiluminescent analytical system (Remax Electronic Instrument Limited Co., Xi'an, China). A three-electrode configuration was used with a Pt wire, Ag/AgCl electrode and GCE served as the counter electrode, reference electrode and working electrode, respectively. ECL detection was accomplished in 0.1 M PBS (pH 7.4) containing 0.10 M KCl and 3.0 mM H_2O_2 and scanned from 0 to – 1.0 V. The voltage of the PMT was set at -750 V.

Synthesis of CdS:Eu QDs

The CdS:Eu QDs were prepared according to our previous work with some modification.[21] Briefly, 112.5 μL of 0.08 M $Eu(NO_3)_3$ solution was added to 30 mL of aqueous solution containing $Cd(NO_3)_2 \bullet 4H_2O$ (0.1683 g) under stirring and heated to 70 °C. Then a freshly prepared solution of $Na_2S \bullet 9H_2O_2$ (0.7205 g) in 30 mL of ultrapure water was injected, and orange-yellow precipitates were obtained instantly. The reaction was held at 70 °C for 3 h with continuous refluxing. The final reaction precipitates were centrifuged and washed thoroughly with absolute ethanol three times, followed by washing with ultrapure water to get rid of any Eu^{3+} and other ions remaining outside the clusters. Then the resulting precipitate was ultrasonically dispersed into water for centrifugation to collect the upper yellow solution of CdS:Eu QDs. The final solution could be rather stable for 1 month when stored in a refrigerator at 4 °C.

Preparation of CdS:Eu QDs film

The GCE was polished in sequential order with 1.0, 0.3, and 0.05 μm alumina before the surface modification. Then the GCE was thoroughly rinsed with water; sonicated in ethanol and ultrapure water in turn; and finally, dried in air. The CdS:Eu QDs film was achieved by dropping 10 μL of the CdS:Eu QDs solution onto the pretreated surface of the GCE and evaporated in air at room temperature. Finally, the CdS:Eu QDs-modified GCE was stored in 0.1 M NaCl + 0.1 M PBS (pH 7.4) for characterization and further use.

Preparation of H-RGO-Au

H-RGO was prepared according to a reported procedure.[22,23] Briefly, 5 mL GO (2 mg/mL) was added into 35 mL ultrapure water. After ultrasonication, 60 μL ammonia solution, 10 mg hemin and 10 μL hydrazine solution were added to the mixture. The solution was heated at 60 °C for 4 h and was centrifugally separated (10000 rpm, 25 min). Then after washing it was dried in vacuo to obtain hemin-reduced graphene oxide (H-RGO).

Then H-RGO-Au was synthesized by reduction $HAuCl_4$ in situ with $NaBH_4$ and ascorbic acid (AA) in the presence of H-RGO. 0.25 mM, 10 mL $HAuCl_4$ was mixed with 10 mL 0.25 mM sodium citrate solution for preparation the seed solution of Au NPs. 0.3 mL fresh solution of $NaBH_4$ (0.1 M) was then injected into the mixed solution under vigorous stirring. When the solution color changed to pink, the seed solution was aged at 27 °C for 2 h before use. To prepare the growth solution, 45 mL 0.25 mM $HAuCl_4$, together with 0.5 g CTAB and 2.8 mg H-RGO product were gently mixed at room temperature, with addition of 0.25 mL 0.1 M AA. The solution became colorless from dark-yellow. Following this, 0.5 mL prepared seed solution was injected into this solution and vigorous stirring at 27 °C for 12 h. Then Au NPs were in situ grown on the surface of H-RGO to form H-RGO-Au NPs.

Preparation of H-RGO-Au/Con A

To prepare H-RGO-Au /Con A, 0.5 mL H-RGO-Au NPs were mixed with 50 μL 0.05% PDDA solution under ultrasonic for 40 min, and then centrifuged. The precipitate was scattered in 400 μL PBS and 100 μL Con A solution (50 μg L^{-1}) was added under gently stirring for 1 h. After centrifugation and washing, the pellet was re-suspended in 500 μL PBS containing 2% BSA and stored at 4 °C for use.

Fabrication of the ECL cytosensing system

The CdS:Eu QDs modified GCE was immersed in 1.0 mL of 0.1 M NaCl + 0.1 M PBS (pH 7.4) containing 1.5 mM MPA for 3 h at 4 °C for assembly of MPA. Then, the terminal carboxylic acid groups of the GCE-CdS:Eu/MPA were activated by treated with 0.1 M imidazole-HCl buffer (pH 6.8) containing 20 mg of EDC and 10 mg of NHS for 1 h. Then, after washing off the excess EDC and NHS, the biosensor was modified by drop-coating of 10 μL 1.5 mg mL^{-1} Con A for incubation for 2 h. Subsequently, 2 wt % BSA solution was introduced for 40 min for the purpose of blocking the nonspecific active binding sites of the CdS:Eu QDs. Finally, the electrode (marked as GCE-CdS:Eu/Con A) was washed by PBS and stored in 4 °C when not used.

Cell Culture and Treatment.

The K562 cell line, derived from a patient with chronic myeloid leukemia, was kindly provided by the Medicine School of Tsinghua University, Beijing, China. K562 cells were cultured in RPMI 1640 medium (GIBCO) supplemented with fetal calf serum (10%, Sigma), penicillin (100 μg mL^{-1}), and streptomycin (100 μg mL^{-1}) at 37 °C in a humidified atmosphere of 5% CO_2. The cells in exponential growth phase were collected and

separated from the medium by centrifugation at 1000 rpm for 5 min and then washed with sterile phosphate buffer saline (PBS, pH 7.4) twice. The sediment was resuspended in sterile PBS containing 1.0 mM Ca^{2+} and Mn^{2+} to obtain a homogeneous cell suspension. Here, the divalent cations Ca^{2+} and Mn^{2+} were required for the activity of Con A binding to cell surface mannose. Cell number was determined using a Petroff-Hausser cell counter (U.S.A.).

ECL measurements

Different concentrations of K562 cells (10 μL) containing 1.0 mM Ca^{2+} and Mn^{2+} were dropped onto the surface of the modified electrode and incubated at 37 °C for 40 min. Subsequently, the electrode was washed thoroughly with 0.1 M PBS (pH 7.4) to remove excess K562 cells and then dropped 10 μL H-RGO-Au NPs/Con A solution consisting of 1.0 mM Ca^{2+} and Mn^{2+} and incubated at 37 °C for 60 min. The sensor was finally washed again with 0.1 M PBS (pH 7.4) to remove the unbound H-RGO-Au /Con A bioconjugates, followed by the measurement of ECL. ECL detection was accomplished with the electrodes in each step in contact with 0.1 M PBS (pH 7.4) containing 0.10 M KCl and 3.0 mM H_2O_2 and scanned from 0 to – 1.0 V. The voltage of the PMT was set at -750 V in the process of detection.

Results and discussion

Characterization of the GO, H-RGO, H-RGO-Au and CdS:Eu QDs

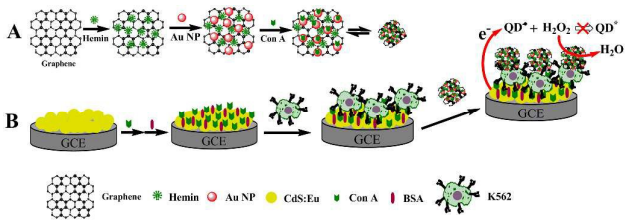

Scheme 1 Schematic illustration of (A) the preparation procedure of H-RGO-Au /Con A, and (B) the developed ECL cytosensing platform.

As shown in Scheme 1A, the synthesis process of H-RGO-Au contains two steps. First, hemin-modified GO (H-RGO) was prepared by heating a mixture of hemin and GO to reflux in ammonia in the presence of hydrazine. During this process, GO was reduced by hydrazine to form a composite of H-RGO by π-π interaction. And then, H-RGO-Au was obtained by reduction of $HAuCl_4$ to get Au nanoparticles on the surface of the H-RGO. The successful synthesis of H-RGO, H-RGO-Au and CdS:Eu QDs were first imaged by TEM. Fig. 1A showed a layer of GO with a wrinkled and folded morphology, while in TEM image of H-RGO (Fig. 1B), some aggregated hemin particles could be found on the surface of RGO. After further decoration of Au NPs, the TEM images in Fig. 1C showed that the Au NPs are densely dispersed on the surface of H-RGO and the size of the generated Au NPs was estimated to be about 10 nm. The CdS:Eu QDs used in this article were synthesized by doping Eu^{3+} ions into CdS QDs, and the average size of the prepared CdS:Eu QDs was showed to be about 6 ± 1 nm, which was demonstrated in Fig. 1D. The composition of CdS:Eu QDs was further confirmed by means of selected area energy dispersive X-ray analysis (SAEDX, Fig. 1E).

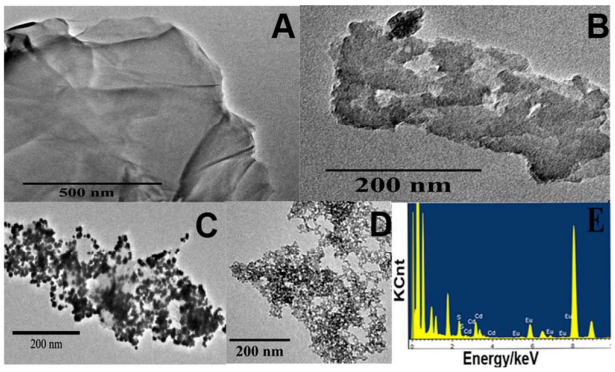

Fig. 1 TEM images of GO (A), H-RGO (B), H-RGO-Au composites (C) , CdS:Eu QDs (D) and the SAEDX analysis of CdS:Eu QDs(E).

Fig. 2A is the UV/Vis absorption spectra of aqueous dispersions of GO, hemin, Con A, H-RGO-Au NPs, H-RGO and H-RGO-Au/Con A. As shown in curve a, we could find that GO exhibits a strong peak centered at approximately 233 nm and a shoulder peak at 300 nm corresponding to π-π* transitions of the aromatic C=C band and n–π* transitions of the C=O band, respectively. The spectrum of the hemin solution contains a strong peak at 388 nm attributed to the Soret band of hemin (curve b). After introduction of hemin on the surface of GO, the maximum of the Soret band of hemin is found red shift from 388 to 413 nm (curve e), the reason is the adsorption of hemin molecule on GO driven by π-π stacking interactions between the porphyrin moiety and RGO. After further decoration of Au NPs (curve d), a new absorption peak appears at approximately 520 nm, which correspond to the surface plasmon absorption of Au NPs. When Con A was conjugated to the H-RGO-Au NPs, a 275 nm absorption peak was observed besides the other visible absorption peaks (curve f). The absorption band of 275 nm is assigned to the protein Con A (curve c). And this indicates the generation of H-RGO-Au/Con A.

The electrocatalytic activity of synthetic H-RGO-Au was compareded with traditional hemin-graphene components (H-RGO) with the cyclic voltammograms (CVs) and the current response at -0.65 V was chosen as the analytical signals. Fig. 2B shows the current absolute value of this H-RGO-Au ternary composite is 3.42×10^{-5}A (curve b), which exhibits a higher electrocatalytic activity for the reduction of H_2O_2 than that of traditional H-RGO (2.25×10^{-5}A, curve a).

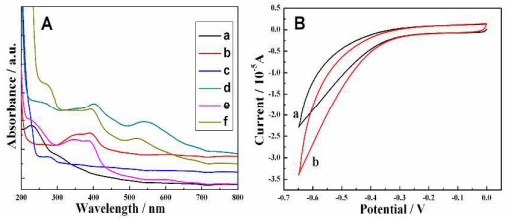

Fig. 2 (A) UV–vis spectrum of GO (curve a), hemin(curve b), Con A (curve c), H-RGO-Au NPs (curve d), H-RGO (curve e) and H-RGO-Au NPs-Con A (curve f); (B) CVs of 3.0 mM H_2O_2 with addition of (a) H-RGO and (b) H-RGO-Au with the same concentration.

Characterization of the ECL cytosensing

Scheme 1B represents the scheme of the proposed ECL cytosensing for K562 cell detection based on H-RGO-Au/Con A composite. As is described, the CdS:Eu QDs were coated onto the surface of glassy carbon electrode (GCE) to form a well-dispersed nanofilm, then the Con A was assembled on the surface of nanofilm for the specific recognition of cell-surface glycans.[24-27] After blocking nonspecific active binding sites using BSA and further capturing of cells, the electrode was incubated with the previously prepared H-RGO-Au/Con A composite to form a sandwich type system based on the binding affinity between Con A and mannose groups.

Every step of the fabrication process of this ECL cytosensor was continuously monitored by electrochemical impedance spectroscopy (EIS, Fig. 3A) and ECL (Fig. 3B). In Fig. 3A, the bare electrode displayed an almost straight line (curve a), which was characteristic of a diffusion process. While CdS:Eu QDs were assembled on the electrode surface, the electron–transfer resistance (Ret) increased obviously (curve b), which indicated that the CdS:Eu QDs were immobilized on the electrode surface and decreased the electron-transfer efficiency. And the further addition of the Con A layer and following incubation of K562 cells resulted in a larger Ret (curve c and d). And this is mainly due to the poor electroconduction of biomolecules which results in steric hindrance and then inhibits the interfacial charge transfer. However, after following conjugated nanoprobe of H-RGO-Au/Con A onto the surface of K562 cells through specific interaction between membrane glycans and the Con A, an obvious of Ret decreases was appeared, which indicates that the synthesized H-RGO-Au/Con A possessed high conductivity, good electron transfer efficiency and excellent biocompatibility (curve e).

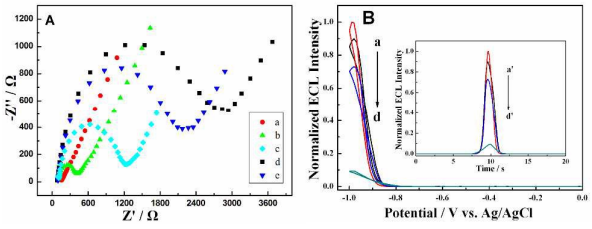

Fig. 3 (A) EIS of (a) bare GCE; (b) GCE-CdS:Eu; (c) GCE-CdS:Eu/Con A; (d) GCE-CdSA:Eu/Con A /K562; (e) GCE-CdS:Eu/Con A/K562/ H-RGO-Au/Con A in 0.1 M KCl solution containing 5.0 mM $K_3[Fe(CN)_6]/K_4[Fe(CN)_6]$; (B) The normalized ECL-potential curves of (a) GCE-CdS:Eu; (b) GCE-CdS:Eu/Con A; (c) GCE-CdS:Eu/Con A/K562; (d) GCE-CdS:Eu/Con A/K562/H-RGO-Au/Con A, inset: the corresponding ECL intensity-time behavior: a′ to a; b′ to b; c′ to c; d′ to d. ECL detection buffer: 0.1 M PBS (pH 7.4) containing 0.10 M KCl and 3.0 mM H_2O_2. Scan rate, 100 mV s^{-1}.

At the same time, ECL signals at each immobilization step were also recorded to characterize the fabrication process of the cytosensing platform. As shown in Fig. 3B, the GCE–CdS:Eu QDs showed a strong, stable cathodic ECL emission in the presence of coreactant H_2O_2 when the potential of electrodes becomes sufficiently negative (curve a). And then, the ECL signal decreased successively with sequential assembly of Con A (curve d) and capture of K562 cell (curve e) due to the obstruction of electron transfer from these poor electroconductive biomolecules on the electrode surface. After following conjugation of H-RGO-Au/Con A on the designed biosensor, the ECL signal obviously decreased due to the H-RGO-Au catalyst with the higher electrocatalytic reduction ECL coreactant (H_2O_2) could efficient quenching of ECL from CdS:Eu QDs. These results confirmed the successful preparation of the cytosensing.

ECL quenching mechanism by H-RGO-Au

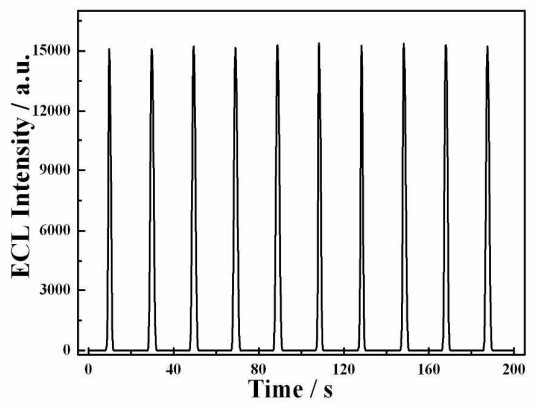

Fig. 4 ECL emission from CdS:Eu QDs-modified GCE under a continuous cyclic potential scan for 10 cycles. ECL detection buffer: 0.1 M PBS (pH 7.4) containing 0.10 M KCl and 3.0 mM H_2O_2. Scan rate, 100 mV s^{-1}.

In our design, glassy carbon electrode (GCE) was modified by drop-coating of 10 μL CdS:Eu QDs composites and used as ECL emitter. During the cathodic potential scan, the CdS:Eu QDs were reduced to $CdS:Eu^{\bullet}$, and the coreactant H_2O_2 could react with $CdS:Eu^{\bullet}$ to obtain an excited state (CdS:Eu*). This state emitted light in the aqueous solution to produce the stable and high ECL signal (Fig. 4). The ECL mechanism was listed as Eqs. (1) - (3).[28] Upon addition of Hemin-RGO-Au, the ECL intensity decreased, which could be attributed to the electrochemical reduction of Hemin-RGO-Au. The reduced Hemin-RGO-Au then chemically reduced the H_2O_2 and resulted to the efficient consumption of the coreactant. The process could be described by the following mechanism (Eqs. (4) and (5)).[29,30]

$$CdS{:}Eu + e^- \longrightarrow (CdS{:}Eu)^{-\bullet} \quad (1)$$

$$2(CdS{:}Eu)^{-\bullet} + H_2O_2 \longrightarrow 2(CdS{:}Eu)^* + 2OH^- \quad (2)$$

$$(CdS{:}Eu)^* \longrightarrow CdS{:}Eu + h\nu \quad (3)$$

$$Hemin[Fe(III)]\text{-}RGO\text{-}Au + e^- \longrightarrow Hemin[Fe(II)]\text{-}RGO\text{-}Au \quad (4)$$

$$2Hemin[Fe(II)]\text{-}RGO\text{-}Au + H_2O_2 \longrightarrow 2Hemin[Fe(III)]\text{-}RGO\text{-}Au + 2OH^- \quad (5)$$

Optimization of Detection Conditions

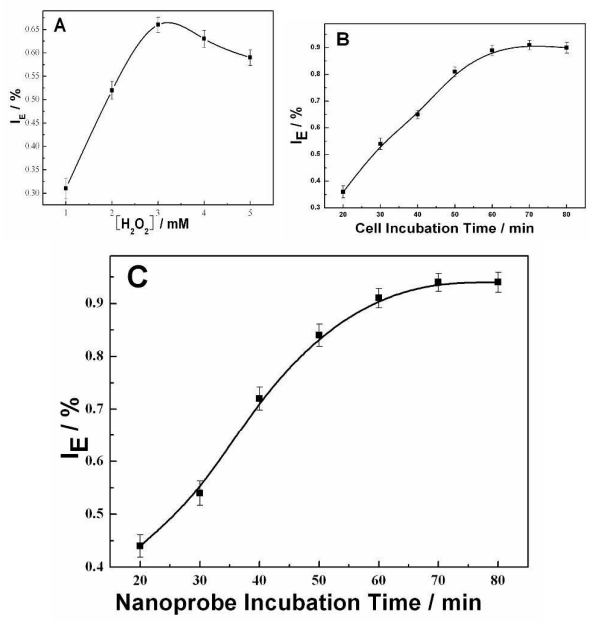

Fig. 5 Optimization of: (A) the concentrations of H_2O_2; (B) cell incubation time; and (C) nanoprobe incubation time. ECL detection buffer: 0.1 M PBS (pH 7.4) containing 0.10 M KCl and 3.0 mM H_2O_2. Scan rate, 100 mV s^{-1}.

The parameters including the concentration of H_2O_2, the incubation time of capturing cells and the incubation time of specific recognition of H-RGO-Au/Con A by N-glycan were studied in the following experiments. Here quenching efficiency was employed defined as I_E = 1- I/I_0, where I and I_0 are the ECL intensity of the presence and absence of K562 cells, respectively. As shown in Fig. 5A, the quenching efficiency was enhanced with increased concentration of H_2O_2, and the quenching efficiency reached the highest when 3.0 mM H_2O_2 was used, and then showed a sharp decrease. Hence, 3.0 mM H_2O_2 was selected as the optimized concentration of H_2O_2. The incubation time was also an important factor for cell capture on the GCE-CdS:Eu/Con A and the specific recognition of H-RGO-Au/Con A by N-glycan presented on the captured cell surface. The ECL intensity was found to increase with the increasing cell incubation time and tend to a constant value at 70 min (Figure 5B), suggesting the saturated capture of K562 cells under this incubation time. And the incubation time of specific recognition of H-RGO-Au/Con A by N-glycan presented on the captured cell surface showed the similar tend as that of cell incubation time.(Figure 5C). Hence, 70 min was selected for the optimal conditions for cell capture and nanoprobes incubation.

Detection of the K562 cancer cells

The performance of the designed ECL cytosensor for K562 cell detection was verified using different cell concentrations under the same experimental conditions during the biosensing process. As shown in Fig. 6, ECL intensity decreased as the K562 cell concentration increased, and the ECL quenching efficiency (IE) was found to be logarithmically related to the concentration of K562 cell in the range from 4.8×10^2 to 5.0×10^5 cells mL^{-1} (R = 0.997, inset in Fig. 6). The detection limit was detected to be 480 cells mL^{-1}. Considering that 10 µL cell suspension was used for incubation in our experiment, the presented cytosensor actually achieved the detection of about 5 cells, which was comparable with that of 8 K562 cells (linear response range from 100 to 10^7 cells mL^{-1}) and 5 T47D cells (linear response range from 50 to 10^7 cells mL^{-1}) by lectin-tagged quantum dot[31] or Fe_3O_4@nanocage core-satellite hybrid nanoparticles[32] with electrochemical cytosensing. And much lower than that of 12 HCCC-9810 cells (linear response range from 6.0×10^2 to 1.0×10^7 cells mL^{-1}) and 38 K562 cells (linear response range from 1.0×10^2 to 5.0×10^7 cells mL^{-1}) with chemiluminescence[33] and colorimetric[34] cytosensing. From this, we could conclude that the designed H-RGO-Au could be broadly exploited its application as a novel tracing tag for a QD-based ECL biosensing. Meanwhile, the relative standard deviation (RSD) on five different GCE was 5.8% for K562 cells (1× 10^3 cells mL^{-1}), thus giving an acceptable precision and fabrication reproducibility of the proposed ECL cytosensing.

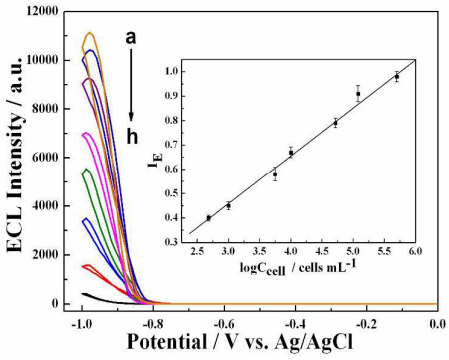

Fig. 6 ECL signal responses for K562 cells of (a) 0, (b) 4.8×10^2, (c) 1.0×10^3, (d) 5.6×10^3, (e) 1.0×10^4, (f) 5.2×10^4, (g) 1.2×10^5, and (h) 5.0×10^5. Inset: linear relationship between ECL quenching efficiency (I_E) and the logarithm of K562 concentration, three measurements for each point.

Monosaccharide inhibition assay

Finally, a monosaccharide inhibition assay was performed to validate the specificity of the interaction between Con A and cell-surface glycan in the following experiment. First, the Con A modified GCE-CdS:Eu QDs nanofilm (GCE-CdS:Eu/Con A) was pretreated with excess Nacetylglucosamine (GlcNAc) or mannose (Man) under appropriate conditions, and then incubation with K562 cells and H-RGO-Au/Con A composite in sequence. And another GCE-CdS:Eu/Con A electrode without treatment were used as comparison. Results in Fig. 7 showed that the electrode treated with Man (Curve b) presented a similar ECL signal as that of GCE-CdS:Eu/Con A electrode

(Curve a) in the presence of 3.0 mM H_2O_2. While when the GCE-CdS:Eu/Con A was pre-treated with GlcNAc, a greatly depressed signal appeared after cell capture and further incubation of H-RGO-Au/Con A (Curve c). Above results prove that the attached Con A on the GCE-CdS:Eu did not recognize GlcNAc and therefore did not influence the ability of the system to capture cells. However, the active sites of Con A on the GCE-CdS:Eu could be occupied by pretreated excess monosaccharide (Man), inhibiting the bind with mannosyl groups on the K562 cells. These results verified that Con A could recognize glycan on the cell surface and could realize the detection of K562 cells expressing glycan based on this proposed cytosensor system through the application of simple electrochemical techniques.

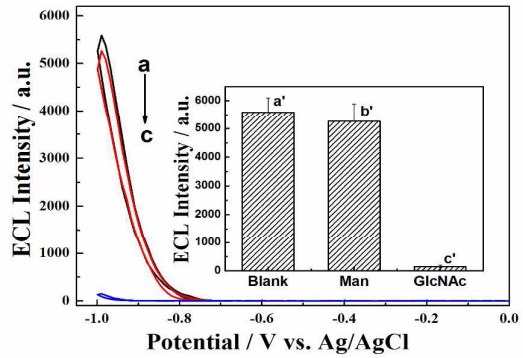

Fig. 7 The ECL-potential curves of GCE-CdS:Eu/Con A (Curve a) treated with (Curve b) Man and GlcNAc (Curve c). Insert is the corresponding histogram obtained from the above three electrodes. ECL detection buffer: 0.1 M PBS (pH 7.4) containing 0.10 M KCl and 3.0 mM H_2O_2. Scan rate, 100 mV s^{-1}.

Conclusions

In conclusion, we have presented the ternary composite of H-RGO-Au which could efficiently electro-catalyze the reduction of H_2O_2. Based on the consumption of ECL coreactant H_2O_2 and the binding recognization between Con A and cell-surface N-glycans, a simple and sensitive ECL cytosensing platform was proposed which innovatively integrated the advantages of electrocatalytic H-RGO-Au composite and ECL technology in biosensing process. It also provides new opportunities for ultrasensitive monitoring of underlying biological processes related to cancers using simple electrochemical method.

Acknowledgements

This work was supported by the National Natural Science Foundation of China (Grant Nos. 21405072, 21505065), the Project of Shandong Province Higher Educational Science and Technology Program (J14LC14 and J14LC15), the Shandong Provincal Natural Science Foundation (ZR2014BL022, ZR2014BL023, and ZR2014BL026), and State Key Laboratory of Analytical Chemistry for Life Science (SKLACLS1407).

Notes and references

1 Z. F. Ding, B. M. Quinn, S. K. Haram, L. E. Pell, B. A. Korgel and A. J. Bard, *Science*, 2002, **296**, 1293-1297.
2 M. M. Richter, *Chem. Rev.*, 2004, **104**, 3003-3036.
3 W. Miao, *Chem. Rev.*, 2008, **108**, 2506-2553.
4 L. Z. Hu and G. B. Xu, *Chem. Soc. Rev.*, 2010, **39**, 3275-3304.
5 H. Zhou, J. Liu and S. S. Zhang, *TrAC-Trend Anal. Chem*., 2015, **67**, 56-73.
6 H. J. Wang, R. Yuan, Y. Q. Chai, Y. L. Cao, X. X. Gan, Y. F. Chen and Y. Wang, *Biosens. Bioelectron*., 2013, **43**, 63-68.
7 Y. Chen, M. L. Yang, Y. Xiang, R. Yuan and Y. Q. Chai, *Nanoscale*, 2014, **6**, 1099-1104.
8 L. L. Li , K. P. Liu , G. H. Yang, C. M. Wang , J. R. Zhang and J. J. Zhu, *Adv. Funct. Mater.*, 2011, **21**, 869-878.
9 M. L. Yang, Y. Chen, Y. Xiang, R. Yuan and Y. Q. Chai, *Biosens. Bioelectron*., 2013, **50** , 393-398.
10 S.Y. Deng, J. P. Lei, Y. Huang, X.N. Yao, L. Ding and H. X. Ju, *Chem. Commun*., 2012, **48**, 9159-9161.
11 D. J. Lin, J. Wu, F. Yan, S. Y. Deng and H. X. Ju, *Anal. Chem.*, 2011, **83**, 5214-5221.
12 E. Yoo, T. Okata, T. Akita, M. Kohyama, J. Nakamura and I. Honma, *Nano Lett.*, 2009, **9**, 2255-2259.
13 Y. Liang, Y. Li, H. Wang, J. Zhou, J. Wang, T. Regier and H. Dai, *Nat. Mater.*, 2011, **10**, 780-786.
14 J. Mao, R. H. Guo and L. T. Yan, *Biomaterials.*, 2014, **35**, 6069-6077.
15 M. Liu, H. Zhao, S. Chen, H. Yu and X. Quan, *ACS Nano*., 2012, **6**, 3142-3151.
16 H. Chen, Y. Li, F. Zhang, G. Zhang and X. Fan, *J. Mater. Chem*., 2011, **21**, 17658-17661.
17 Y. L. Dong, H. G. Zhang, Z. U. Rahman, L. Su, X. J. Chen, J. Hu and X. G. Chen, *Nanoscale*, 2012, **4**, 3969-3976.
18 W. K. Chee, H. N. Lim, N. M. Huang and I. Harrison, *RSC Adv*., 2015, **5**, 68014-68051
19 H. Song, Y. Ni and S. Kokot, *Anal.Chim.Acta*., 2013, **788**, 24-31.
20 X. Lv and J. Weng, *Sci.Rep*., 2013, **3**, 3285-3294.
21 H. Zhou, Y.Y. Zhang, J. Liu, J. J. Xu and H. Y. Chen, *J. Phys. Chem. C*., 2012, **116**, 17773–17780.
22 J. Liu, X. Y. Xin, H. Zhou and S. S. Zhang , *Chem. Eur. J.*, 2015, **21**, 1908-1914.
23 L. Z. Gao, J. Zhuang, L. Nie, J. B. Zhang, Y. Zhang, N. Gu, T. H. Wang, J. Feng, D. L. Yang, S. Perrett and X. Yan, *Nat. Nanotechnol.*, 2007, **2**, 577-583.
24 Y. Z. Wang, Z. H. Chen, Y. Liu and J. H. Li, *Nanoscale*, 2013, **5**, 7349-7355.
25 W. Cheng, L. Ding, S. J. Ding, Y. B. Yin and H. X. Ju, *Angew. Chem. Int. Ed.*, 2009, **48**, 6465-6468.
26 H. Y. Liu, S. M. Xu, Z. M. He, A. P. Deng and Z. Z. Zhu, *Anal. Chem*., 2013, **85**, 3385-3392.
27 Z. H. Chen, Y. Liu, Y. Z. Wang, X. Zhao and J. H. Li, *Anal. Chem*., 2013, **85**, 4431-4438.
28 L. Deng, Y. Shan, J.-J. Xu and H.-Y. Chen, *Nanoscale*, 2012, **4**, 831-836.
29 S. Y. Deng, J.P. Lei, Y. Huang, Y. Cheng and H.X. Ju, *Anal. Chem*., 2013, **85**, 5390-5396.
30 H. Zhou, Y.-Y. Zhang, J. Liu, J.-J. Xu and H.-Y. Chen, *Chem. Commun*., 2013, **49**, 2246-2248.
31 L. Ding, W. Cheng, X. J. Wang, S. J. Ding and H. X. Ju, *J. Am. Chem. Soc*., 2008, **130**, 7224-7225.
32 T. T. Zheng, Q. F. Zhang, S. Feng, J.-J. Zhu, Q. Wang and H. Wang, *J. Am. Chem. Soc*., 2014, **136**, 2288-2291.
33 E. Han, L. Ding, R. C. Qian, L. Bao and H. X. Ju, *Anal. Chem*., 2012, **84**, 1452-1458.
34 S. G. Ge, F. Liu, W. Y. Liu, M. Yan, X. R. Song and J. H. Yu, *Chem. Commun*., 2014, **50**, 475-477.

Graphical Abstract

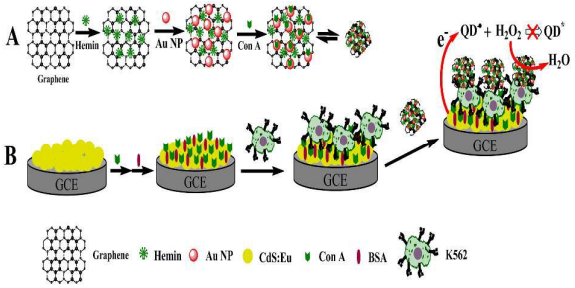

A sensitive ECL cytosensor was designed using H-RGO-Au ternary composite with high electrocatalytic activity for the H_2O_2.